EUKARYOTIC CELL, Oct. 2010, p. 1455–1465 Vol. 9, No. 10
1535-9778/10/$12.00 doi:10.1128/EC.00109-10

Spitzenkörper, Exocyst, and Polarisome Components in *Candida albicans* Hyphae Show Different Patterns of Localization and Have Distinct Dynamic Properties▽†

Laura A. Jones‡ and Peter E. Sudbery*

Department of Molecular Biology and Biotechnology, University of Sheffield, Western Bank, Sheffield S10 2TN, United Kingdom

Received 7 May 2010/Accepted 31 July 2010

During the extreme polarized growth of fungal hyphae, secretory vesicles are thought to accumulate in a subapical region called the Spitzenkörper. The human fungal pathogen *Candida albicans* can grow in a budding yeast or hyphal form. When it grows as hyphae, Mlc1 accumulates in a subapical spot suggestive of a Spitzenkörper-like structure, while the polarisome components Spa2 and Bud6 localize to a surface crescent. Here we show that the vesicle-associated protein Sec4 also localizes to a spot, confirming that secretory vesicles accumulate in the putative *C. albicans* Spitzenkörper. In contrast, exocyst components localize to a surface crescent. Using a combination of fluorescence recovery after photobleaching (FRAP) and fluorescence loss in photobleaching (FLIP) experiments and cytochalasin A to disrupt actin cables, we showed that Spitzenkörper-located proteins are highly dynamic. In contrast, exocyst and polarisome components are stably located at the cell surface. It is thought that in *Saccharomyces cerevisiae* exocyst components are transported to the cell surface on secretory vesicles along actin cables. If each vesicle carried its own complement of exocyst components, then it would be expected that exocyst components would be as dynamic as Sec4 and would have the same pattern of localization. This is not what we observe in *C. albicans*. We propose a model in which a stream of vesicles arrives at the tip and accumulates in the Spitzenkörper before onward delivery to the plasma membrane mediated by exocyst and polarisome components that are more stable residents of the cell surface.

Polarized growth of fungi requires that a supply of secretory vesicles is delivered along cytoskeletal tracks to the site of cell expansion (for reviews, see references 13, 29, 30, and 31). Fusion of these membrane-bound vesicles with the plasma membrane allows the necessary expansion of the plasma membrane and releases the enzymes and raw materials for the synthesis of new cell wall material and the remodeling necessary to allow this newly synthesized material to be inserted into the existing cell wall. The process of polarized growth has been extensively studied in the budding yeast *Saccharomyces cerevisiae* and provides a model for studying the process in other fungi (for a review, see reference 20). Post-Golgi vesicles travel to sites of polarized growth along actin cables (23). Actin cables are nucleated at sites of polarized growth by the formin Bni1 facilitated by a multiprotein complex called the polarisome, which consists of Spa2, Bud6, and Pea1(5, 22, 24, 27). The motive force for vesicle transport is provided by Myo2, a class V myosin, complexed to its regulatory light chain Mlc1 (22, 26). At the plasma membrane, secretory vesicles dock with a second multiprotein complex called the exocyst before fusion with the plasma membrane (14, 15, 32, 33), mediated by v-SNARES on the vesicle and t-SNARES on the membrane. The exocyst is an octomeric complex composed of Sec3, Sec5, Sec6, Sec8, Sec10, Sec15, Exo70, and Exo84 (21). It is thought that Sec3 and a fraction of the Exo70 pool are localized at sites of polarized growth independently of the actin cytoskeleton (3, 6). The other exocyst subunits and the remainder of the Exo70 pool are thought to be transported to sites of polarized growth on secretory vesicles, where together with Sec3 and Exo70 they form the exocyst complex (3). Secretory vesicles exit the Golgi apparatus, travel toward sites of polarized growth, and dock with the exocyst by use of the Rab-type GTPase Sec4 in its GTP-bound form, which is activated by its GEF, Sec2 (12, 19, 35, 36). In the *S. cerevisiae* cell cycle, polarized growth is initially directed toward the bud tip in young buds (17). Growth subsequently becomes isotropic in larger buds before being directed toward the mother bud neck during cytokinesis at the end of the cell cycle. Accordingly, polarisome and exocyst components localize to the tips of young buds (7, 27, 28).

The rate of hyphal tip extension is much greater than that of the growth of a yeast or pseudohyphal bud. In rich yeast extract-peptone-dextrose (YEPD) medium, *Candida albicans* hyphae extend at the rate of 0.25 μm min^{-1}, compared to 0.0625 μm min^{-1} in yeast buds and 0.125 μm min^{-1} in pseudohyphal cells (P. Sudbery unpublished observations). In hyphae of filamentous fungi, a structure called a Spitzenkörper is present at the tip, which is rich in secretory vesicles (8, 9, 11, 29, 34). It is believed that the Spitzenkörper acts as a vesicle supply center (VSC) (1). This model proposes that the Spitzenkörper is maintained at a fixed distance from the hyphal tip. Vesicles radiate out in equal directions to fuse with the plasma membrane, so that more vesicles per unit area fuse with the hyphal tip itself than with other parts of the hyphae. Mathematical

* Corresponding author. Mailing address: Department of Molecular Biology and Biotechnology, University of Sheffield, Western Bank, Sheffield S10 2TN, United Kingdom. Phone: 44 (0)1142226186. Fax: 44 (0)1142222800. E-mail: P.Sudbery@shef.ac.uk.

† Supplemental material for this article may be found at http://ec.asm.org/.

‡ Present address: Faculty of Life Sciences, Michael Smith Building, Oxford Road, Manchester M13 9PT, United Kingdom.

▽ Published ahead of print on 6 August 2010.

TABLE 1. Strains used in this study

Strain	Genotype	Reference
BWP17	*URA3*::λ*imm434*/*URA3*::λ*imm434his1*::*hisG*/*his1*::*hisG arg4*::*hisG*/*arg4*::*hisG*	37
Sec6-YFP	BWP17 *SEC6*/*SEC6-YFP*::*URA3*	This study
Exo70-YFP	BWP17 *EXO70*/*EXO70-YFP*::*URA3*	This study
Sec3-YFP	BWP17 *SEC3*/*SEC3-YFP*::*URA3*	This study
Exo84-YFP	BWP17 *EXO84*/*EXO84-YFP*::*URA3*	This study
Sec4-GFP	BWP17 *SEC4*/*GFP-SEC4*::*URA3*	18
Sec8-YFP	BWP17 *SEC8*/*SEC8-YFP*::*URA3*	This study
Exo70-YFP	BWP17 *EXO70*/*EXO70*::*YFP*	This study
Sec4-GFP/Exo70-YFP	BWP17 *EXO70*/*EXO70-YFP*::*HIS1*/*SEC4*/*GFP-SEC4*::*URA3*	This study
Mlc1-YFP	BWP17 *MLC1*/*MLC1-YFP*::*URA3*	4
Spa2-GFP	BWP17 *SPA2*/*SPA2-YFP*::*URA3*	4
Sec2-YFP/sec2Δ	BWP17 *SEC2-YFP-URA3*/*sec2*::*HIS1*	2
Sec4-GFP/Exo70-YFP	BWP17 *SEC4*/*GFP-SEC4-URA3*/*EXO70*/*EXO70-YFP-HIS1*	This study

modeling shows that this explains the distinctive shape of hyphal tips.

In order to investigate the mechanism of polarized growth in the hyphae of *Candida albicans*, we previously determined the localization of Mlc1-yellow fluorescent protein (YFP) and the polarisome components Bud6-YFP and Spa2-YFP (4). We found that in hyphae, polarisome components localized to a surface crescent, as they did in young yeast buds and the tips of elongated pseudohyphal buds. However, in hyphae Mlc1-YFP localized to a bright spot, which at least in some hyphae was clearly inside the tip, rather than at the surface, and which appeared spherical in three-dimensional reconstructions. We concluded that this represented a Spitzenkörper. In some hyphae Mlc1-YFP also localized to a surface crescent, similar to the pattern displayed by polarisome components. This observation suggested that the Spitzenkörper and polarisome were separate structures, both of which were present at hyphal tips, but that only the polarisome was present at the bud tips of pseudohyphae and yeast. Moreover, the dual localization of Mlc1-YFP to a crescent and a spot suggested that Mlc1 may be present in both structures.

While *S. cerevisiae* has proved to be an excellent model to investigate the molecular genetics of polarized growth, it is less optimal to study the spatial organization of the molecular components because polarized growth of the bud is restricted to a short period after bud emergence when the nascent bud is small. Thus, there has been little effort to investigate the fine detail of the spatial organization of the different components of the polarization machinery beyond noting that they localize to sites of polarized growth. In this study we exploited the opportunities afforded by the continuous polarized growth of *C. albicans* hyphae to clarify the relationship between the Spitzenkörper, polarisome, and exocyst, which cooperate to mediate the extreme polarized growth of hyphae. We show that the vesicle-associated marker Sec4 also localizes to a Spitzenkörper-like structure, confirming the existence of a vesicle-rich area corresponding to a Spitzenkörper at the hyphal tip. We show that exocyst components such as Sec3, Sec6, Sec8, Exo70, and Exo84 localize to a surface crescent, so the exocyst, like the polarisome, is also a spatially separate structure from the Spitzenkörper. We used three independent strategies to investigate the dynamic properties of these structures. Fluorescence recovery after photobleaching (FRAP) was used to measure the rate at which new proteins arrived at the tip. Fluorescence loss in photobleaching (FLIP) was used to measure the rate at which proteins exited the tip. Cytochalasin A was used to disrupt actin cables, allowing the persistence of proteins at the tip to be measured after the supply of new proteins was blocked. In each case we found that Spitzenkörper components Sec4, Sec2, and Mlc1 were highly dynamic, while the polarisome component Spa2 was stable. Intriguingly, exocyst components showed intermediate dynamic properties, suggesting that they are delivered to the tip on vesicles but that not all vesicles carry a complement of exocyst components. We suggest that these data are consistent with a model in which a stream of vesicles arrives at the tip and accumulates in the Spitzenkörper before onward delivery to the plasma membrane mediated by exocyst and polarisome components that are more stable residents of the cell surface.

MATERIALS AND METHODS

Strains. All strains were derived from BWP17 (*ura3*Δ/Δ *arg4*Δ/Δ *his1*Δ/Δ). Genes encoding homologues of *S. cerevisiae* exocyst components were identified by two-way BLAST searches, the results of which were supported by annotation in the *Candida* genome database (www.candidagenome.org/). C-terminal fusions were generated as previously described using pFA-YFP plasmids carrying the appropriate *URA3*, *ARG4*, or *HIS1* genes (10, 25). Full genotypes of the strains are provided in Table 1, and the oligonucleotides used are listed in Table S1 in the supplemental material.

Growth conditions. Hyphal growth was induced by growing yeast cells at 25°C overnight to saturation in YEPD (2% glucose, 2% Difco Bacto peptone, and 1% Difco Bacto yeast extract plus 80 mg liter^{-1} uridine). The stationary-phase culture was washed with distilled water and inoculated at a 1:20 dilution into synthetic defined (SD) medium (consisting of 0.67% yeast nitrogen base [Difco], 2% [wt/vol] glucose, and 80 mg liter^{-1} each of histidine, uridine, and arginine in phosphate-buffered saline [PBS], pH 7.0) plus 20% calf serum (Sigma-Aldrich) and incubated at 37°C. Under these conditions, hyphae evaginate after 35 to 40 min. For live-cell imaging in FRAP and FLIP experiments, cells were grown on agar pads incorporating SD medium as described previously (2).

Cytochalasin A (Sigma Aldrich) was used at working concentration of 10 μM from a stock concentration of 1 mg ml^{-1} in dimethyl sulfoxide (DMSO). Typically, 5 μl of the stock solution was added to 1 ml of cells. Control experiments showed that the DMSO alone had no effect on hyphal growth or localization of the fluorescent proteins.

Microscopy. Images of exocyst components fused to YFP and green fluorescent protein (GFP)-Sec4 localization were made using a Delta Vision Spectris 4.0 RT microscope (Applied Precision Instruments, Seattle, WA) using an Olympus 100× UPlanAPo NA 1.35 lens (Olympus, Tokyo, Japan). Images were acquired and deconvolved with Softworx software. To visualize the cell outline in fluorescent images, cells were counterstained with 1 μg/ml calcofluor white (Fluorescent Brightener 28; Sigma-Aldrich, St. Louis, MO).

All FRAP and FLIP experiments were carried out on hyphae actively growing on the surface of an agar pad in a concavity slide maintained at 37°C by a heated

TABLE 2. *C. albicans* homologues of *S. cerevisiae* exocyst components

S. cerevisiae protein, ORF	Best hit in *C. albicans* genome	E value[a]	Assigned gene name in CGD[b]
Sec3, YER008C	Orf19.2911	2.5e−18	*SEC3*
Sec6, YIL068C	Orf19.5463	1.5e−47	*SEC6*
Sec8, YPR055W	Orf19.3647	1.2e−93	*SEC8*
Exo70, YJL085W	Orf19.6512	3.5e−48	*EXO70*
Exo84, YBR102C	Orf19.135	3.2e−30	*EXO84*

[a] E values are from BLAST searches using the *S. cerevisiae* protein sequence to probe the *C. albicans* genome.
[b] CGD, *C. albicans* genome database (www.candidagenome.org).

stage and environment chamber (Pecon GmbH, Erbach, Germany). FRAP and FLIP experiments were carried out using a Zeiss LSM 510 Meta confocal microscope running release 4.0 SP2 software. The 514-nm HFT laser and the long-pass 530 filter were used to image YFP, and the 488 HFT laser and long-pass 505 filter were used to image GFP. Photobleaching was carried out using the argon/2 laser, which was set up with tube power at 6.0 Å and used at 45% of the total power and with the region of interest (ROI) positioned to expose the hyphal tip of the bleached cell (FRAP) or a strip 1 μm wide located approximately 3 μm behind the tip (FLIP). A nonbleached tip in the same field served as a control for bleaching due to image acquisition in the recovery period. Average image intensity was measured using LSM software for the experiments shown in Fig. S3 in the supplemental material and using NIH Image J for the experiments shown in Fig. 3 and 4 and in Fig. S2 in the supplemental material. Raw values were subject to a subtraction of background. Values were then corrected for bleaching due to image acquisition in the recovery period according to the proportional loss of intensity in the control tip at the same time point, which was set to 100% prebleach. For each time point the fraction of fluorescence recovered (FRAP) or lost (FLIP) was calculated according to the formula $(I_t - I_b)/(I_0 - I_t) \times 100\%$, where t = time in seconds, I_0 = intensity prebleaching, I_b = intensity immediately postbleach, and I_t = intensity at time t. Prism software (GraphPad Software Inc.) was then used to fit the best curve to a plot of time versus fraction fluorescence recovered. In all experiments analyzed, the best fit was to a nonlinear curve with a one-phase exponential. The same software was used to generate the bar chart and carry out t tests for pairwise comparisons shown in Fig. 3.

RESULTS

Exocyst components localize to a surface crescent, but Sec4 localizes to a Spitzenkörper-like structure. We carried out BLAST searches to identify *C. albicans* orthologues of *S. cerevisiae* Sec3, Sec6, Sec8, Exo70, and Exo84 proteins (Table 2). Except for Sec3, all proteins identified were of similar length, and the similarity extended across the full length of the protein. Although the similarity was less clear in the case of Orf19.2911, the putative *C. albicans* Sec3 orthologue, it has been shown that this gene can functionally complement an *S. cerevisiae sec3* mutant and localizes to hyphal tips (18). We generated C-terminal YFP fusions of each of these *C. albicans* exocyst orthologues. In each case the exocyst component clearly localized to a surface crescent in the tips of essentially all hyphae examined. Figure 1 shows the pattern of localization of representative hyphal tips for each exocyst protein. Figure S1 in the supplemental material shows a field of cells expressing Sec3-YFP, with each tip enlarged to show the consistency of the localization pattern. A similar consistency was seen in the localization patterns of the other exocyst components. Although there were bright spots of fluorescence within the crescent, these were clearly qualitatively different from the spot-like localization of Sec4, which we discuss further below. We also obtained similar results for a putative Sec15 homologue (R. Lane and P. Sudbery, unpublished observations). Thus, like the polarisome (4), exocyst components localize to a surface crescent and not the Spitzenkörper.

An N-terminal GFP-Sec4 fusion has previously been shown to localize to hyphal tips, but no attempt was made to distin-

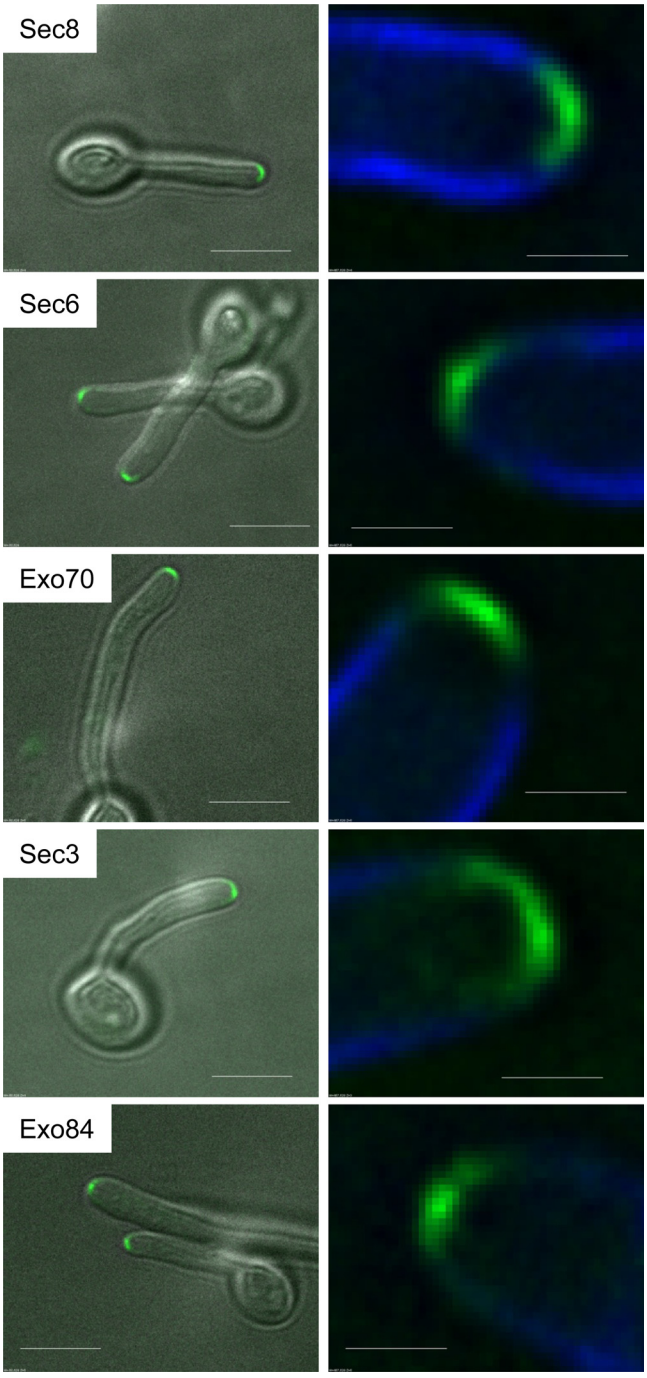

FIG. 1. Exocyst components localize to a surface crescent. Hyphae expressing the indicated fusions to YFP were imaged 90 min after stationary-phase yeast cells were induced to form hyphae. Images are projections of the deconvolved Z-stack. All images are representative. Scale bars: left panels, 5 μm; right panels, 1 μm.

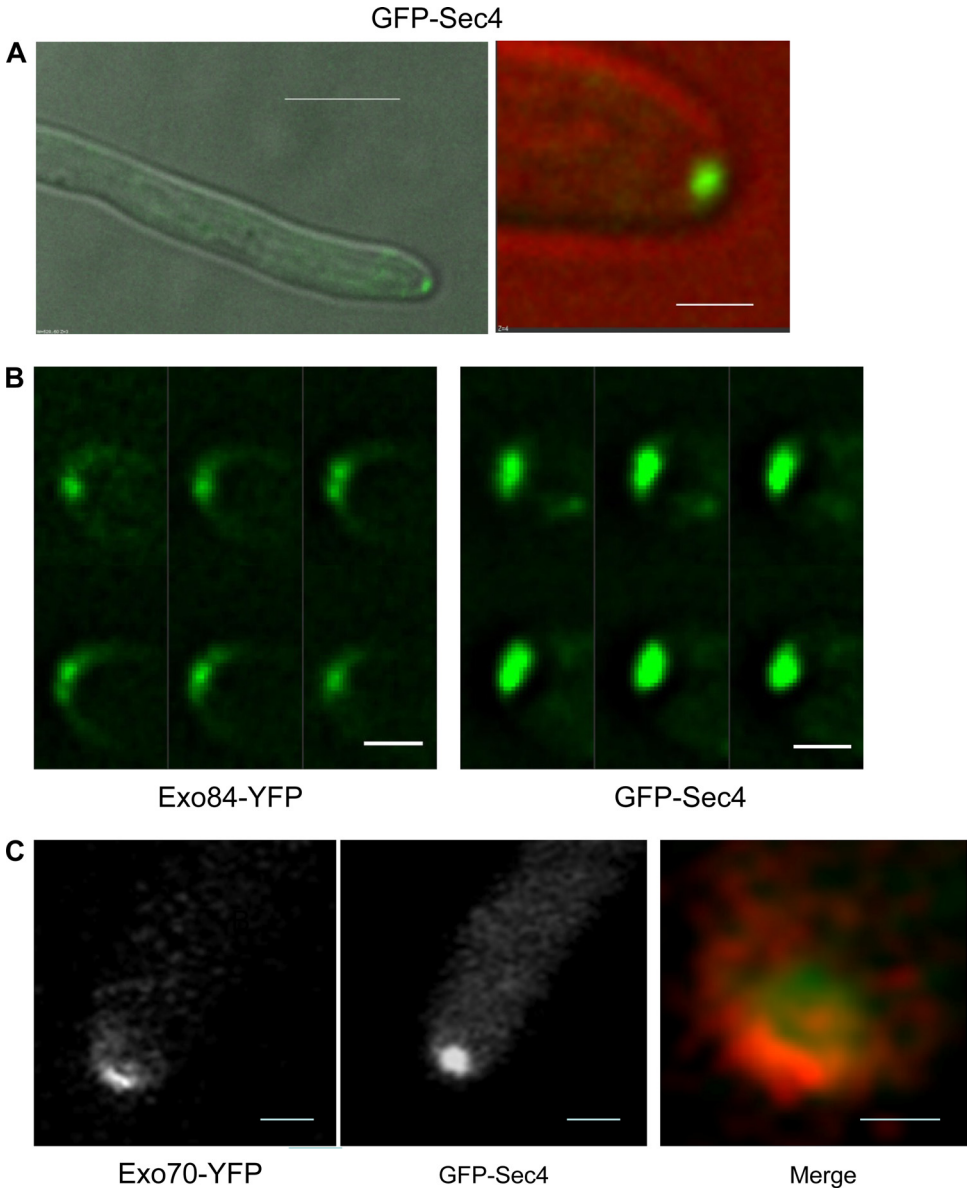

FIG. 2. Sec4 localizes to a apical spot distinct from the crescent of the exocyst components. (A) A hyphal cell expressing GFP-Sec4 was imaged at 90 min after induction from a stationary-phase yeast culture. The left image shows the merge of the differential interference contrast (DIC) and GFP channels at low magnification, and the right image shows an enlargement of the tip, with the DIC false colored red to allow the GFP image to be clearly seen. Scale bars: left, 5 μm; right, 1 μm. (B) Montage showing the image from individual Z-stacks of GFP-Sec4 and Exo84-YFP. Images were taken with 0.2-μm vertical separation. Exposure and processing of both sets of images were identical. Scale bars, 1 μm. (C) Strains expressing Exo70-YFP and GFP-Sec4 were imaged using a Zeiss LSM Meta 510 laser scanning confocal microscope. GFP-Sec4 is false colored red in the merged image, in which the tip has been enlarged to facilitate visualization of the different pattern of localization. The 514-nm HFT laser was used to excite YFP, and the 488 HFT laser was used for GFP. The emission was gated to 500 to 530 nm for GFP images and 530 to 570 for YFP images. To test for bleedthrough, images were recorded using single YFP- and GFP-tagged strains using these gates. Bleedthrough of YFP signal with GFP settings was effectively excluded, but some weak fluorescence was apparent from GFP with YFP settings. However, this was so low compared to the genuine YFP signal that the localization of Exo70-YFP could be easily visualized and is different from that of GFP-Sec4. Scale bars: left and center, 1 μm; right, 0.5 μm.

guish whether its localization was to a spot or crescent (18). We have reexamined this strain (kindly provided by Yue Wang) and found that GFP-Sec4 localizes to a spot, rather than a crescent, in essentially all hyphae examined. (Fig. 2A; see Fig. S1 in the supplemental material). Since Sec4 is a recognized secretory vesicle-associated marker (19), this supports the notion that the spherical structure previously observed in *C. albicans* hyphae is indeed a vesicle-rich Spitzenkörper. We have also obtained a similar result with Sec2, the GEF for Sec4 (2). As pointed out above, bright spots were sometimes visible in the crescent-like localization of exocyst components. However, the localization of GFP-Sec4 was qualitatively different. Figure 2B shows a montage of the individual Z-planes of GFP-Sec4 and Exo84-YFP. The large GFP-Sec4 spot is clearly visible

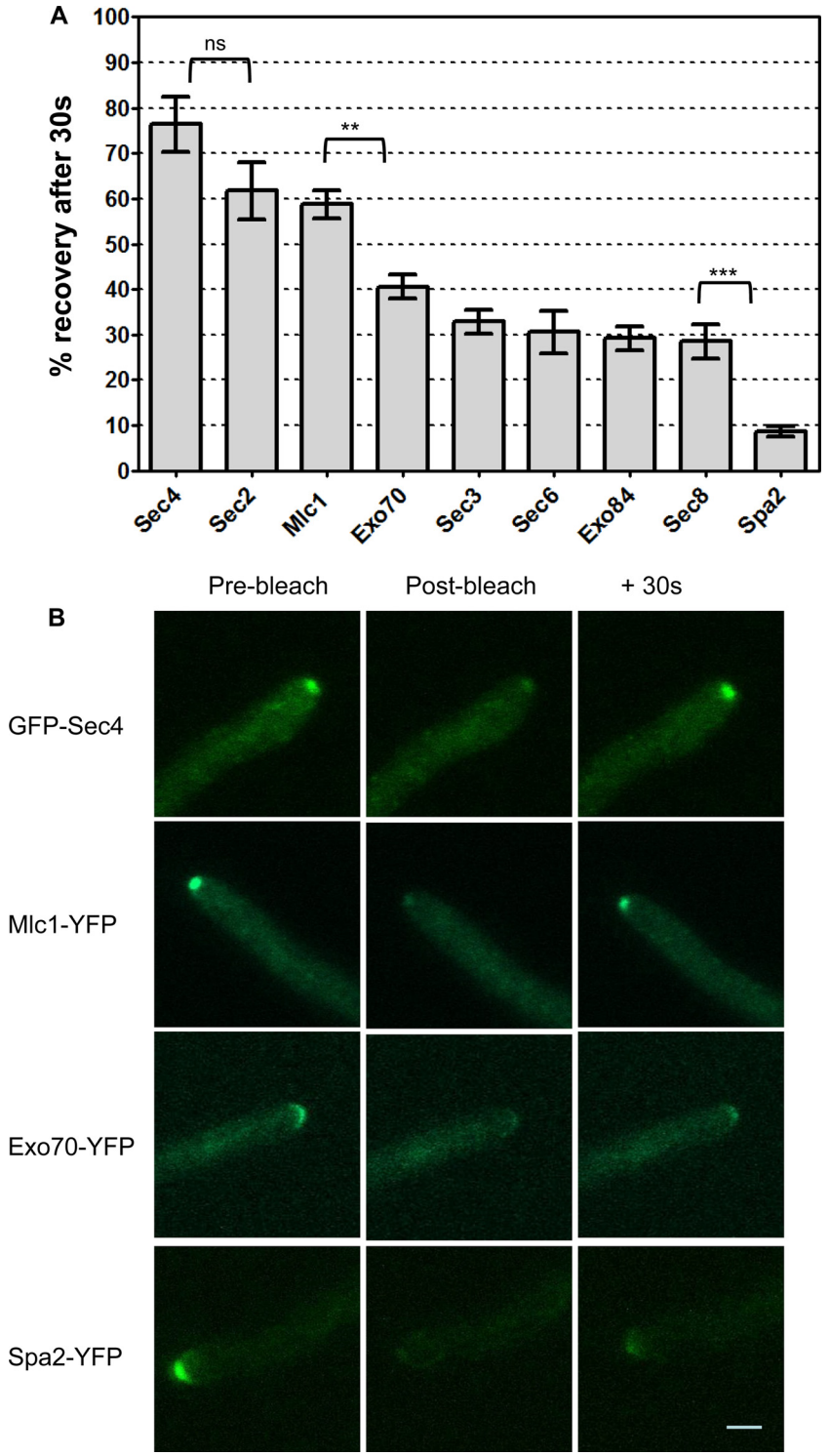

FIG. 3. Fluorescence recovery of Spitzenkörper, exocyst, and polarisome components. Strains expressing the indicated proteins fused to YFP or GFP (Sec4) were grown on surface agar concavity slides under hypha-inducing conditions for 90 min. A minimum of 10 hyphal tips of each strain were bleached with a Zeiss LSM 510 as described in Materials and Methods, and images were recorded immediately before bleaching (prebleach), 1.5 s after bleaching (postbleach), and at 30-s intervals after bleaching (+30s). (A) The average fluorescence intensity was measured in each tip, and the percentage of fluorescence lost by bleaching that was recovered after 30 s was calculated according to the formula $(I_{30} - I_b)/(I_0 - I_b) \times 100$, where I_{30} = intensity at 30 s after bleaching, I_b = postbleach intensity, and I_0 = prebleach intensity. Error bars are standard errors of the means. Results of pairwise *t* tests are shown above the brackets. ***, $P = 0.0001$; **, $P = 0.0014$; ns, difference not significant ($P = 0.1$). (B) Representative images of individual hyphal tips at prebleach, postbleach, and +30 s. Scale bar, 2 μm.

throughout the Z-stack, whereas the bright spots in Exo84-YFP are confined to individual focal planes and the surface crescent.

Similar investigations with *Ashbya gosspyii* found that the pattern of localization of exocyst proteins and the polarisome protein Spa2 depended upon hyphal extension rates (16): in fast-growing hyphae these proteins localized to a spot, while in slow-growing hyphae they localized to a surface crescent. The observation that the pattern of localization of exocyst and polarisome components is dependent on growth rate in *A. gosspyii* raises the question of whether the different patterns of localization that we have observed in *C. albicans* may simply be the result of variation in growth rates between strains carrying different fluorescent protein fusions. This question may be addressed by determining the pattern of localization of Spitzenkörper, polarisome, or exocyst components in the same cell, thus removing growth rate as a variable. Indeed, we previously showed that Spa2-YFP localized to a crescent and Mlc1-cyan fluorescent protein (CFP) to a Spitzenkörper in the same hypha (4). However, the quantum efficiency of CFP when fused to *C. albicans* proteins is very low, making visualization of the target protein difficult. The spectral characteristics of YFP and GFP prevent the signals being distinguished by the Delta Vision wide-field epifluorescence microscope that we routinely use. However, YFP and GFP signals can be distinguished with a Zeiss laser scanning META confocal microscope using appropriate lasers for excitation and setting appropriate limits to the adjustable emission channels (see the legend Fig. 2). By this means we visualized Exo70-YFP and GFP-Sec4 in the same cell and confirmed that Exo70-YFP localized to a crescent and GFP-Sec4 to a spot (Fig. 2C).

FRAP experiments show that Spitzenkörper, exocyst, and polarisome components have different dynamic properties. We carried out fluorescence recovery after photobleaching (FRAP) experiments to investigate whether the different patterns of localization of exocyst, polarisome, and Spitzenkörper components are reflected in different dynamic properties. In such experiments the rate of fluorescence recovery, measured by the time constant τ, reports the rate at which new fluorescent components replace bleached components (the smaller the value, the more rapid the recovery). When the recovery curve reaches a plateau, the fraction of the original fluorescence regained is a measure of the fraction that is mobile. The use of FRAP was complicated by the time span of several minutes that it took for exocyst components to recover, while Spitzenkörper components recovered within a single minute. To accommodate these different time scales, we acquired postbleach images every 5 s for GFP-Sec4, Mlc1-YFP, and Spa4-YFP (see Fig. S3 in the supplemental material) and every 30 s for GFP-Sec4 Mlc1-YFP, Sec8-YFP, Sec2-YFP, Bud6-YFP, Sec3-YFP, and Spa2-YFP (see Fig. S3 in the supplemental material). The derived values for τ, half-time ($t_{1/2}$), and mobile fraction (see Table S2 in the supplemental material) indicate that Sec4 and Mlc1 are most dynamic, the exocyst components were less dynamic, and the polarisome component Bud6 was least dynamic.

The time span of several minutes for exocyst components to show full recovery made it difficult to generate enough reliable replicates for statistical analysis, because the hyphal tip would frequently grow in the Z dimension, rendering it out of focus in the postbleach images. Refocusing during this period would distort the results, as the additional image acquisition required would itself cause bleaching of the fluorophore being measured. (In *C. albicans*, YFP and GFP are very sensitive to photobleaching.) Although it was possible to calculate τ values from these data, the confidence limits were large, which made comparisons between strains problematic (see Table S2 in the supplemental material). Since we had established that exocyst components did eventually recover their full fluorescence (see Table S2 in the supplemental material), the fraction recovered after 30 s is dependent only on the recovery rate and not on the mobile fraction. Thus, we used Sec4 as a benchmark to compare the fraction of fluorescence recovered in a single image acquired after 30 s in a minimum of 10 replicate hyphal tips (20 in the case of Mlc1-YFP). Moreover, the single postbleach image acquired in this protocol has the additional benefit that a bleaching correction was not necessary. The results are shown in Fig. 3A. Consistent with the previous experiments, GFP-Sec4 showed the most rapid recovery. The next-highest rate was shown by Mlc1-YFP and Sec2-YFP, both of which, like Sec4, localize to the Spitzenkörper. Although the difference in the rates of recovery for Sec2 and Sec4 fell short of statistical significance in a two-tailed *t* test ($P = 0.1$), the pattern was reproduced in previous experiments and is likely to be real. The exocyst components, Exo70-YFP, Sec3-YFP, Exo84-YFP, Sec8-YFP, and Sec6-YFP, formed a group with intermediate recovery rates. The difference in the rates of recovery of Mlc1-YFP and Exo70-YFP, the most dynamic exocyst component, was significant ($P = 0.0014$). The polarisome component Spa2-YFP showed the lowest recovery rate; the difference between the rates of recovery of Spa2-YFP and Sec8-YFP was highly significant ($P = 0.0001$). Figure 3B shows images of hyphal tips prebleach, postbleach, and after 30 s of recovery. GFP-Sec4, Mlc1-YFP, Exo70-YFP, and Spa2 are shown to represent each class of protein described above with respect to the rate of recovery. Taken together, these results show that the different patterns of localization of vesicle-associated proteins that localize to the Spitzenkörper, such as Sec4, Mlc1, and Sec2, and exocyst and polarisome components is reflected in the different dynamic properties of these proteins.

The Spitzenkörper is in dynamic equilibrium between vesicles entering and leaving. FRAP experiments determine the rate at which a bleached protein is exchanged for an unbleached protein. Thus, in the present context, these experiments measure the rate at which new, unbleached proteins arrive at the tip. The rate at which proteins are lost from the tip can be measured by a fluorescence loss in photobleaching (FLIP) experiment, in which a strip just behind the tip is continually bleached, ablating the fluorescence of proteins before they arrive at the tip. Fluorescence declines because fluorescence on vesicles leaving the tip is not replaced by the fluorescence of newly arriving proteins. GFP-Sec4 or Spa2-YFP was grown under hypha-inducing conditions and repeatedly bleached at 1-s intervals in a strip just behind the tip. To correct for bleaching during image acquisition after each bleaching event, a field was chosen with two hyphal tips, one of which served as a control. The results are expressed as the fraction of initial fluorescence remaining in the bleached hyphae normalized to the fraction of initial fluorescence remaining in the control tip (Fig. 4). In the case of GFP-Sec4, fluo-

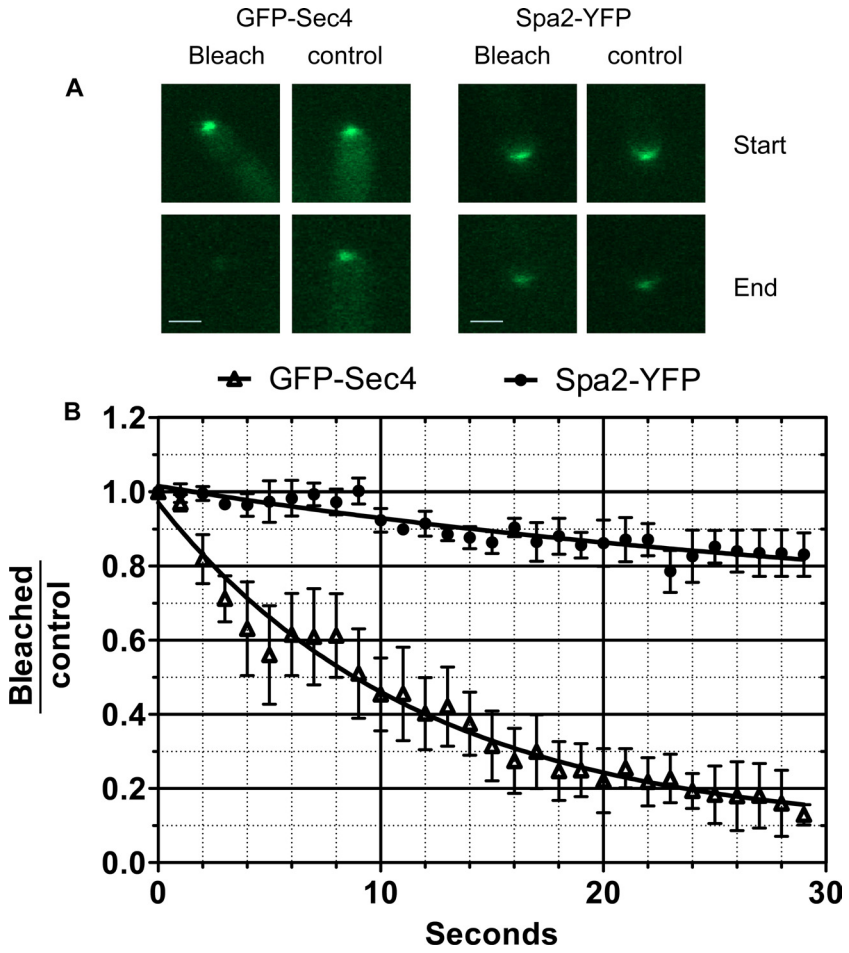

FIG. 4. FLIP experiments show that GFP-Sec4 is more dynamic than Spa2-YFP. Fields of GFP-Sec4 or Spa2-YFP with two growing tips were chosen. A strip, approximately 3 μm behind one tip and 1 μm wide, was bleached at 1-s intervals for 30 s, and an image was acquired after each bleaching event. The other unbleached tip served as a control. (A) Images of experimental and control tips at the start and end of the experiment. Fluorescence declines in all tips due to bleaching during image acquisition, but GFP-Sec4 in the experimental tip has a visibly lower intensity at the end of the experiment than the control tip. Scale bars, 1 μm. (B) The fraction of initial fluorescence remaining in control and experimental tips was determined at each time point as described in Materials and Methods. The graph plots the ratio of fluorescence remaining in the bleached tip compared to that in the control tip. $n = 3$ for GFP-Sec4; $n = 5$ for Spa2-GFP. Nonlinear curves were fitted with Prism software assuming a one-phase exponential. Error bars are standard errors of the means. Tau values were calculated by Prism software: GFP-Sec4 = 11.7 (95% confidence interval, 8.2 to 20.3); Spa2-YFP = 37.4 (95% confidence interval, 7.6 to ∞).

rescence rapidly declined. The time constant (τ) of the exponential decline was 11.7 s (95% confidence interval, 8.2 to 20.3 s). This value is similar the τ value of 10.6 s (95% confidence interval, 7.5 to 18.0 s) calculated in FRAP experiments (see Table S2 and Fig. S2 in the supplemental material), suggesting that Sec4 in the Spitzenkörper is in a state of dynamic flux, with a constant stream of incoming molecules replacing molecules that exit. In contrast, the fluorescence of Spa2-YFP showed only a modest decline during the course of the FLIP experiments, suggesting that Spa2 is a stable component of the polarisome at the cell surface.

Spitzenkörper components, but not exocyst or polarisome components, depolarize rapidly upon disruption of actin cables. The FRAP and FLIP experiments described above suggest that Sec4 is more dynamic than the exocyst components. If GFP-Sec4 and exocyst components are delivered to the tip along actin cables, then Sec4 should depolarize faster than exocyst components upon disruption of actin cables. To test this prediction, we used cytochalasin A, which disrupt actin cables and leads to tip swelling after 15 min. After the addition of cytochalasin A to liquid cultures, we monitored the persistence of polarized Spitzenkörper, polarisome, and exocyst components. There was a clear difference in the rates of depolarization of Spitzenkörper components and of exocyst and polarisome components. GFP-Sec4 depolarized within 90 s upon addition of cytochalasin A, and the fluorescence dispersed into bright punctate spots distributed throughout the germ tube mother cell (Fig. 5A). The value of 90 s is a maximum figure, representing the shortest time taken after addition of the drug to a liquid culture to withdraw a sample, prepare and mount a slide, and focus and record an image. Mlc1-YFP (Fig. 5B and C) and Sec2-YFP (data not shown) also depolarized rapidly, although after 3 min some polarized material remained, consistent with the slightly slower kinetics of FRAP. In the case of Mlc1-YFP, a faint surface crescent remained in some hyphae (Fig. 5C), which persisted for up to 15 min; this

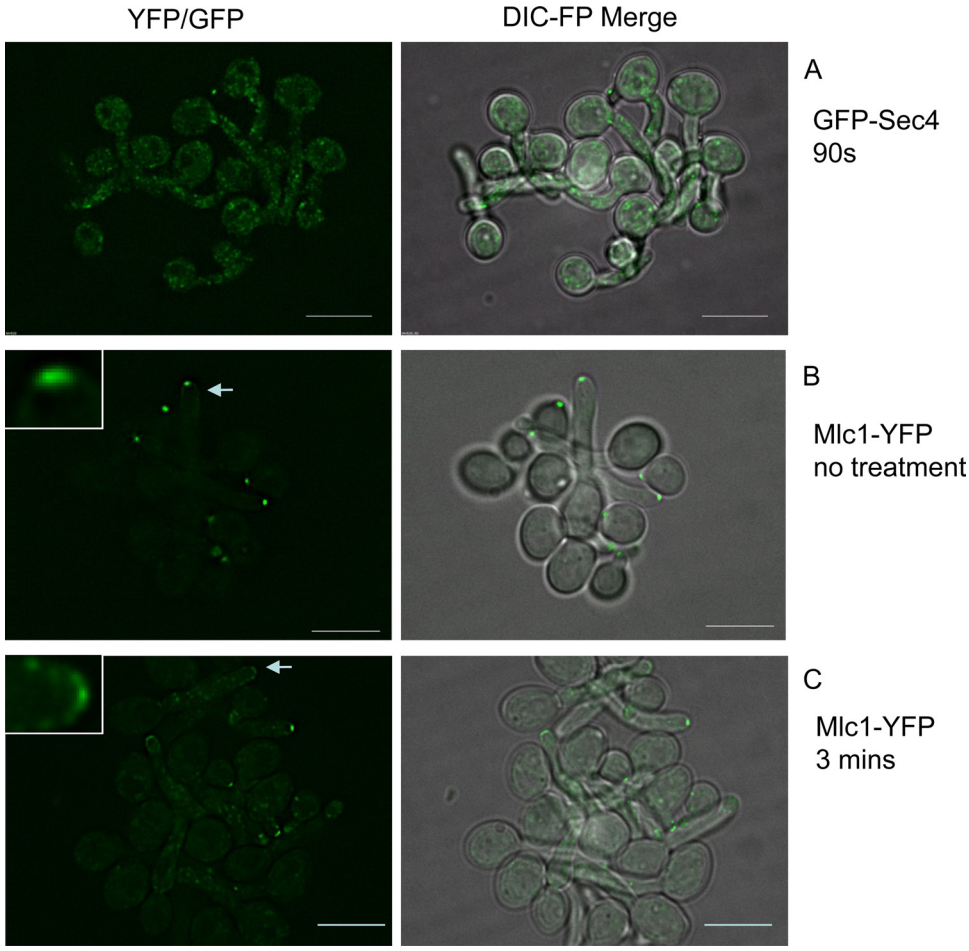

FIG. 5. Spitzenkörper components depolarize rapidly upon disruption of the actin cables with cytochalasin A. Hyphae of the indicated strains were treated with 10 μM cytochalasin A and images recorded after the indicated times. The strain expressing Mlc1-YFP is shown pretreatment, as its localization is not shown elsewhere in this paper. In all hyphae it localizes to a bright subapical spot (e.g., arrowed tip, enlarged in the inset). After 3 min of treatment with cytochalasin A, these have largely disappeared. In some hyphae Mlc1-YFP remains in a fainter surface crescent (e.g., arrowed tip, enlarged in the inset). The experiment was initiated at 60 min after inoculation of stationary-phase yeast cultures into synthetic complete medium plus 20% serum and incubation at 37°C. Scale bars, 5 μm.

may represent Mlc1-YFP present in the polarisome as we previously reported.

In contrast, exocyst and polarisome components were all still fully polarized after 5 min. Sec3-YFP is shown as an example in Fig. 6A. In the case of Sec3, the fluorescence eventually dispersed into punctate spots by 15 min (Fig. 6B). In the case of Spa2, the fluorescence was still clearly visible after 15 min as the tip started to swell (Fig. 6D). In the case of other exocyst components, the fluorescence slowly faded at the tip, but the crescent was still visible as the tip started to swell after 15 min (e.g., Sec8-YFP) (Fig. 6C). Thus, consistent with the FRAP and FLIP experiments, the Spitzenkörper components are in a state of rapid dynamic flux, while the polarisome and Spitzenkörper components are more stable.

DISCUSSION

We previously showed that at the tip of *C. albicans* hyphae, Mlc1-YFP localized to a spot while the polarisome components Spa2 and Bud6 localized to a crescent. We suggested that Mlc1 was localizing to a Spitzenkörper and that this was a spatially distinct structure from the polarisome. Here we extend this work by showing that GFP-Sec4 also localizes to a spot. We describe elsewhere a similar localization pattern for Sec2, the GEF for Sec4 (2). Not only do these observations confirm the existence of a Spitzenkörper in *C. albicans* hyphal tips, but they also show that the Spitzenkörper is indeed rich in secretory vesicles, as suggested by electron microscope images of the Spitzenkörper in other fungal hyphae. We further show that exocyst components localize to a surface crescent, suggesting that the exocyst is a structure that is spatially distinct from the Spitzenkörper. It should be noted that in this work we did not formally assess the functionality of the exocyst-YFP fusions. However, in both *S. cerevisiae* and *A. gosspyii*, all of these fusions have been shown to be functional (16). Moreover, the similar localization patterns of all the exocyst components provide additional confidence that the observations are reliable.

Localization of exocyst and polarisome components has been reported for *A. gosspyii* (16). Upon spore germination, hyphae initially grow at a lower rate than is attained in longer

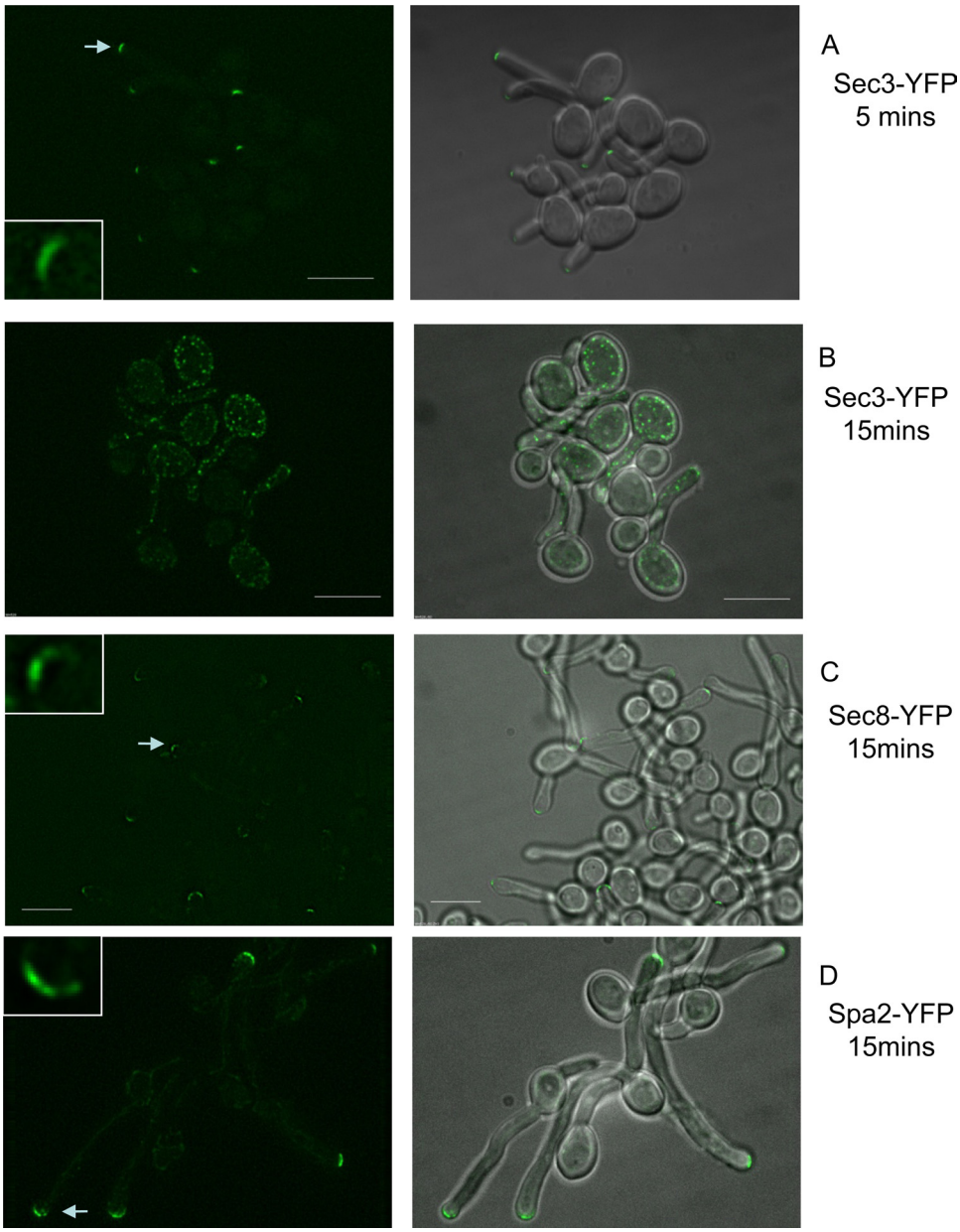

FIG. 6. Exocyst and polarisome components depolarize slowly upon disruption of the actin cables with cytochalasin A. Hyphae of the indicated strains were treated with 10 μM cytochalasin A and images recorded after the indicated times as described in the legend to Fig. 5. Exocyst and polarisome components such as Sec3 are fully polarized at 5 min after treatment. They remain polarized even as the tip starts to swell after 15 min. Arrows indicate hyphal tips enlarged in the insets. Similar results were obtained for all the other exocyst components. Scale bars, 5 μm.

hyphae. It was found that the localization pattern of exocyst components depended on the growth rate. In the slow growth phase, these components localize to a surface crescent as we find in *C. albicans* hyphae. However, at a higher growth rate, both the exocyst and Spa2 were found to localize to the Spitzenkörper. These observations can be reconciled with our observations by considering that hyphal growth in *C. albicans* is analogous to the slow mode of hyphal growth in *A. gosspyii*, so that in both cases exocyst components and Spa2 localize to a crescent. According this scenario, Mlc1, Sec4, and Sec2 would localize to the Spitzenkörper in slow-growing *A. gosspyii* hyphae. Unfortunately, the localization of these components was not reported to allow this prediction to be tested.

Having established that Sec4, Mlc1, and Sec2 localize to a spot whereas polarisome and exocyst components localize to a crescent, we next investigated whether these differences in spatial organization were reflected in different dynamic properties. Three independent experimental strategies confirmed that this was indeed the case. The reliability of conventional FRAP recovery curves was compromised by the time span of several minutes required for full recovery of exocyst and polarisome components and the broad confidence limits on the

estimations of τ. Although we generated such curves and report them in the supplemental material, we consider the fraction of fluorescence recovered by 30 s to be a more reliable guide. It is important to note that the full FRAP curves show that exocyst components did eventually recover 100% of the original fluorescence so that the fraction recovered by 30 s is not limited by the size of the mobile fraction. Both types of FRAP experiment led to the same conclusion that the Spitzenkörper components GFP-Sec4, Mlc1, and Sec2 were more dynamic than the exocyst components, which in turn were more dynamic than the polarisome components Spa2 and Bud6. Among the Spitzenkörper components, GFP-Sec4 appeared to be more dynamic than Mlc1 or Sec2. An explanation for this difference may be that Sec2 may detach from the vesicles after activating Sec4. Similarly, Mlc1 may be released from the Myo2-secretory vesicle complex after it arrives at the Spitzenkörper. In contrast Sec4 may remain on the vesicle until its fusion with the plasma membrane.

The full FRAP curves (see Fig. S2 and S3 and Table S2 in the supplemental material) generated a τ value for GFP-Sec4 (10.7 s) which is very similar to the value reported by Boyd et al. for Sec4 in *S. cerevisiae*. Interestingly, in that study Sec4 also showed a higher recovery rate than exocyst components (3). However, that study reported τ values in the range of 15 to 20 s for exocyst components other than Sec3 and Exo70, which is considerably faster than we observed. Interestingly, the mobile fraction for these exocyst components in *S. cerevisiae* was reported to be on the order of 40%, while we observed that the mobile fraction was close to 100%. An explanation for these differences is that in *C. albicans* exocyst components can be recruited from distant hyphal locations, so that there is a greater reservoir of unbleached components, but it takes longer for them to be recruited. Sec3 has been reported to be recruited independently of the actin cytoskeleton (6), and Boyd et al. (3) reported a slow recovery time for this exocyst subunit. Moreover, Boyd et al. reported a two-phase recovery for Exo70 and suggested that a fraction of the Exo70 pool was recruited independently of actin cables. We did not observe that Sec3 was less dynamic than the other exocyst components We also observed a one-phase recovery of Exo70-YFP. Thus, in *C. albicans* Exo70 and Sec3 appear to be delivered along actin cables. A similar conclusion was reported for these proteins in *A. gossypii* (16).

In addition to the FRAP experiments, we investigated the dynamic properties in two further ways. First, we used FLIP experiments, which determine the rate at which fluorescence declines when the fluorescence of incoming GFP-Sec4 proteins is ablated by bleaching before they arrive at the tip. We interpret this as a measure of the rate at which vesicles exit the tip. However, an alternative explanation is that GFP-Sec4 detaches from the vesicle once it arrives at the Spitzenkörper. Regardless of which interpretation is correct, the FLIP experiment provides an independent measure of the dynamic properties of Sec4. Importantly, the τ value of the recovery in FRAP experiments (10.6 s; 95% confidence limits, 7.5 s to 18.0 s) was very similar to the τ value of the exponential in the FLIP experiments (11.7 s; 95% confidence limits, 8.2 s to 20.3 s). Taken together, the FRAP and FLIP experiments show that the flux of Sec4 molecules entering and leaving the Spitzenkörper is highly dynamic. Spa2 was much less dynamic in the FLIP experiments, confirming the results of the FRAP experiments.

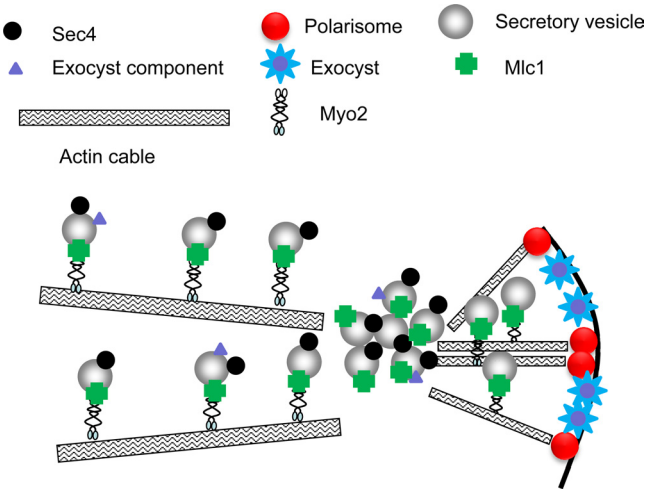

FIG. 7. Model of secretory vesicle delivery to hyphal tips. Secretory vesicles are delivered to the Spitzenkörper along actin cables. All vesicles carry Sec4, but not all carry exocyst components. At the Spitzenkörper, vesicles are loaded onto to actin cables, nucleated by the polarisome, and transported to the cell surface. Upon reaching the surface, vesicles dock with the exocyst. Exocyst components, present on some vesicles, remain at the cell surface to act to tether vesicles arriving at later times.

Finally, we interrupted the supply of molecules to the tip by disrupting actin cables. Again we observed that Sec4, Sec2, and Mlc1 rapidly depolarized upon cytochalasin A treatment. Sec2 was completely depolarized within 90 s. Sec2 and Mlc1 were largely depolarized within 3 min, although some polarized material remained. Interestingly, the remaining polarized Mlc1 protein was distributed in a surface crescent which may represent Mlc1 in the polarisome, as we previously reported (4). In contrast, the polarisome and exocyst components were much more stable. Spa2 remained polarized even as the tip started to swell after 15 min. Exocyst components were also still polarized at this time, although the intensity of the fluorescence had diminished.

A model for hyphal growth. The current paradigm for polarized growth in *S. cerevisiae* considers that exocyst subunits travel to the cell surface on secretory vesicles. (3). If this was the case in *C. albicans*, we would expect that the pattern of localization and dynamic properties of vesicle-associated proteins such as Sec4 and Sec2 would be similar to that of exocyst components. The data presented here provide compelling evidence that this is not the case. Sec4, Sec2, and Mlc1 are clearly transported to the tip on actin cables, where they accumulate in the Spitzenkörper. They are highly dynamic, with a flux of incoming molecules balanced by an outflow, presumably to the cell surface. Exocyst and polarisome components are stably located in a surface crescent. They may be transported to the cell surface on actin cables, but our data leave this question open, as it is possible that the slow depolarization upon cytochalasin A treatment is a secondary consequence of the disruption of actin cables. If they are transported on actin cables, the difference in their dynamic properties compared to those of Spitzenkörper components suggests that only a frac-

tion of vesicles carry exocyst components and that once delivered to the cell surface they remain to act as docking platforms for other incoming vesicles.

Our results suggest that a modified form of the vesicle supply model operates in *C. albicans* hyphae; this model which attempts to explain why proteins such as Sec4 are localized to an apical spot whereas exocyst and polarisome components localize to a surface crescent (Fig. 7). The essential feature of the model is that secretory vesicles marked by Sec4, Sec2, and Mlc1 arrive in a constant stream at the Spitzenkörper along actin cables. The Spitzenkörper is in dynamic balance, with vesicles leaving at the same rate at which they arrive. Post-Spitzenkörper vesicles are delivered to the cell surface along actin cables nucleated by the polarisome located at the cell surface. At the cell surface, they are tethered by exocyst structures which may be carried on the vesicle or may have been left behind after delivery by other vesicles.

ACKNOWLEDGMENTS

This work was funded by BBSRC grant BB/E003273/1. L.A.J. was funded by a Krebs studentship from the University of Sheffield. Delta Vision microscope images were obtained and FRAP and FLIP experiments carried out using the Sheffield University Light Microscope Facility (LMF) supported by Wellcome Trust grant GR077544AIA.

We thank Yue Wang and Rachel Lane for strains.

REFERENCES

1. **Bartnicki-Garcia, S., F. Hergert, and G. Gierz.** 1989. Computer-simulation of fungal morphogenesis and the mathematical basis for hyphal (tip) growth. Protoplasma **153:**46–57.
2. **Bishop, A., R. Lane, R. Beniston, C. Smythe, and P. Sudbery.** 2010. Hyphal growth in Candida albicans requires the phosphorylation of Sec2 by the Cdc28-Ccn1/Hgc1 kinase. EMBO J. [Epub ahead of print.] doi:10.1038/emboj.2010.158.
3. **Boyd, C., T. Hughes, M. Pypaert, and P. Novick.** 2004. Vesicles carry most exocyst subunits to exocytic sites marked by the remaining two subunits, Sec3p and Exo70p. J. Cell Biol. **167:**889–901.
4. **Crampin, H., K. Finley, M. Gerami-Nejad, H. Court, C. Gale, J. Berman, and P. E. Sudbery.** 2005. *Candida albicans* hyphae have a Spitzenkorper that is distinct from the polarisome found in yeast and pseudohyphae. J. Cell Sci. **118:**2935–2947.
5. **Evangelista, M., D. Pruyne, D. C. Amberg, C. Boone, and A. Bretscher.** 2002. Formins direct Arp2/3-independent actin filament assembly to polarize cell growth in yeast. Nat. Cell Biol. **4:**32–41.
6. **Finger, F. P., T. E. Hughes, and P. Novick.** 1998. Sec3p is a spatial landmark for polarized secretion in budding yeast. Cell **92:**559–571.
7. **Finger, F. P., and P. Novick.** 1998. Spatial regulation of exocytosis: lessons from yeast. J. Cell Biol. **142:**609–612.
8. **Girbardt, M.** 1957. Der Spitzenkörper von *Polystictus versicolor*. Planta **50:** 47–50.
9. **Girbardt, M.** 1969. Ultrastructure of apical region of fungal hyphae. Protoplasma **67:**413.
10. **Gola, S., R. Martin, A. Walther, A. Dunkler, and J. Wendland.** 2003. New modules for PCR-based gene targeting in Candida albicans: rapid and efficient gene targeting using 100 bp of flanking homology region. Yeast **20:** 1339–1347.
11. **Grove, S. N., and C. E. Bracker.** 1970. Protoplasmic organization of hyphal tips amoung fungi: vesicles and Spitzenkörper. J. Bacteriol. **104:**989–1009.
12. **Guo, W., D. Roth, C. Walch-Solimena, and P. Novick.** 1999. The exocyst is an effector for Sec4p, targeting secretory vesicles to sites of exocytosis. EMBO J. **18:**1071–1080.
13. **Harris, S. D., N. D. Read, R. W. Roberson, B. Shaw, S. Seiler, M. Plamann, and M. Momany.** 2005. Polarisome meets Spitzenkorper: microscopy, genetics, and genomics converge. Eukaryot. Cell **4:**225–229.
14. **He, B., and W. Guo.** 2009. The exocyst complex in polarized exocytosis. Curr. Opin. Cell Biol. **21:**537–542.
15. **He, B., F. G. Xi, J. Zhang, D. TerBush, X. Y. Zhang, and W. Guo.** 2007. Exo70p mediates the secretion of specific exocytic vesicles at early stages of the cell cycle for polarized cell growth. J. Cell Biol. **176:**771–777.
16. **Köhli, M., V. Galati, K. Boudier, R. W. Roberson, and P. Philippsen.** 2008. Growth-speed-correlated localization of exocyst and polarisome components in growth zones of Ashbya gossypii hyphal tips. J. Cell Sci. **121:**3878–3889.
17. **Kron, S. J., and N. A. R. Gow.** 1995. Budding yeast morphogenesis—signaling, cytoskeleton and cell-cycle. Curr. Opin. Cell Biol. **7:**845–855.
18. **Li, C. R., R. T.-H. Lee, Y. M. Wang, X. D. Zheng, and Y. Wang.** 2007. Candida albicans hyphal morphogenesis occurs in Sec3p-independent and Sec3p-dependent phases separated by septin ring formation. J. Cell Sci. **120:**1898–1907.
19. **Novick, P., M. Medkova, G. Dong, A. Hutagalung, K. Reinisch, and B. Grosshans.** 2007. Interactions between Rabs, tethers, SNAREs and their regulators in exocytosis. Biochem. Soc. Trans. **34:**683–686.
20. **Park, H. O., and E. F. Bi.** 2007. Central roles of small GTPases in the development of cell polarity in yeast and beyond. Microbiol. Mol. Biol. Rev. **71:**48–96.
21. **Pelham, H. R. B.** 2001. SNAREs and the specificity of membrane fusion. Trends Cell Biol. **11:**99–101.
22. **Pruyne, D.** 2002. Role of formins in actin assembly: nucleation and barbed-end association. Science **297:**612–615.
23. **Pruyne, D. W., D. H. Schott, and A. Bretscher.** 1998. Tropomyosin-containing actin cables direct the Myo2p-dependent polarized delivery of secretory vesicles in budding yeast. J. Cell Biol. **143:**1931–1945.
24. **Sagot, I., S. K. Klee, and D. Pellman.** 2002. Yeast formins regulate cell polarity by controlling the assembly of actin cables. Nat. Cell Biol. **4:**42–50.
25. **Schaub, Y., A. Dunkler, A. Walther, and J. Wendland.** 2006. New pFA-cassettes for PCR-based gene manipulation in *Candida albicans*. J. Basic Microbiol. **46:**416–429.
26. **Schott, D., J. Ho, D. Pruyne, and A. Bretscher.** 1999. The COOH-terminal domain of Myo2p, a yeast myosin V, has a direct role in secretory vesicle targeting. J. Cell Biol. **147:**791–807.
27. **Sheu, Y. J., B. Santos, N. Fortin, C. Costigan, and M. Snyder.** 1998. Spa2p interacts with cell polarity proteins and signaling components involved in yeast cell morphogenesis. Mol. Cell. Biol. **18:**4053–4069.
28. **Snyder, M.** 1989. The spa2 protein of yeast localizes to sites of cell-growth. J. Cell Biol. **108:**1419–1429.
29. **Steinberg, G.** 2007. Hyphal growth: a tale of motors, lipids, and the Spitzenkorper. Eukaryot. Cell **6:**351–360.
30. **Sudbery, P. E.** 2008. Regulation of polarised growth in fungi. Fungal Biol. Rev. **22:**44–55.
31. **Sudbery, P. E., and H. Court.** 2007. Polarised growth in fungi, p. 137–166. *In* R. J. Howard and N. A. R. Gow (ed.), Biology of the fungal cell, vol. VIII. Springer-Verlag, Berin, Germany.
32. **Terbush, D. R., T. Maurice, D. Roth, and P. Novick.** 1996. The exocyst is a multi-protein complex required for exocytosis in *Saccharomyces cerevisiae*. EMBO J. **15:**6483–6494.
33. **Terbush, D. R., and P. Novick.** 1995. Sec6, Sec8, and Sec15 are components of a multisubunit complex which localizes to small bud tips in *Saccharomyces cerevisiae*. J. Cell Biol. **130:**299–312.
34. **Virag, A., and S. D. Harris.** 2006. The Spitzenkorper: a molecular perspective. Mycol. Res. **110:**4–13.
35. **Walch-Solimena, C., R. N. Collins, and P. J. Novick.** 1997. Sec2p mediates nucleotide exchange on Sec4p and is involved in polarized delivery of post-Golgi vesicles. J. Cell Biol. **137:**1495–1509.
36. **Walworth, N. C., P. Brennwald, A. K. Kabcenell, M. Garrett, and P. Novick.** 1992. Hydrolysis of GTP by Sec4 protein plays an important role in vesicular transport and is stimulated by a GTPase-activating protein in *Saccharomyces cerevisiae*. Mol. Cell. Biol. **12:**2017–2028.
37. **Wilson, B., D. Davis, and A. P. Mitchell.** 1999. Rapid hypothesis testing in *Candida albicans* through gene disruption with short homology regions. J. Bacteriol. **181:**1868–1874.